EUROPEAN COOPERATION
IN THE FIELD OF SCIENTIFIC
AND TECHNICAL RESEARCH

EURO-COST

SOURCE: Tokyo Institute of Technology

COST 273 TD(03) 119
Paris, France
May 21-23, 2003

High-Resolution Estimation of NLOS Indoor MIMO Channel with Network Analyzer Based System

K. Haneda, J. Takada
1–12–1, O-okayama, Meguro-ku, Tokyo, Japan
Phone: +81 3 5734 3288
Fax: +81 3 5734 3288
Email: haneda@mobile.ss.titech.ac.jp

High-Resolution Estimation of NLOS Indoor MIMO Channel with Network Analyzer Based System

Katsuyuki Haneda, Jun-ichi Takada
Department of International Development Engineering
Tokyo Institute of Technology
2–12–1, O-okayama, Meguro-ku, Tokyo, Japan
Telephone, FAX: +81–3–5734–3288
Email: haneda@mobile.ss.titech.ac.jp

***Abstract*— This report presents a MIMO sounding system dedicated to short range wireless communication. The system can easily be integrated with Vector Network Analyzer (VNA) and other commercial equipments. The advantage of our proposed system is the achievement of completely automatic measurement, while retaining accuracy. Using the system, a double directional measurement campaign in indoor NLOS environment was performed, where the channel was estimated in a deterministic way with the ISI-SAGE algorithm. In the use of ISI-SAGE algorithm, we propose to estimate polarization characteristics for identical path. One of the realizations of the optimum search and initialization with succesive interference cancellation type procedure, which is suitable for large number of sampling available case, is shown as well. The result of the measurement campaign shows the effectiveness of our proposals.**

I. Introduction

The demand for short range wireless communications is increased especially in indoor environments in conjunction with MIMO transmission which increases a channel capacity without having to expand the required bandwidth. To provide an adequate quality of service with these types of communications, it is necessary to evaluate characteristics of the propagation channel over which a communication is operated. There have been many studies on the development of MIMO channel sounding technique or channel sounder (e.g.,[1], [2], [3]). However a channel sounder requires a complex hardware design so some simple configurated system is preferable when we consider the developing time and its cost.

This study proposes an automatic MIMO channel measurement system with simple configuration dedicated to indoor short range communications. The system integrates a few commercial measurement equipment such as Vector Network Analyzer, X-Y positioner, and PC[4]. With the system, we estimate the channel in a deterministic way with the high resolution algorithm, ISI-SAGE[3]. A measurement campaign was performed in indoor NLOS environment in order to evaluate the efficiency of the system. In the campaign, we estimated jointly the parameters of the paths which characterize a propagation, such as direction of arrival (DOA), direction of departure (DOD), time of arrival (TOA), and path gain including polarization. Herein we show a specification of the automatic measurement system and result of the experiment as well as the way of implementation of ISI-SAGE algorithm considering a polarization.

II. MIMO Channel Estimation System

The system we propose is depicted in Fig. 1. One of the antenna aperture is a synthesized uniform rectangular array (SURA), and another is a synthesized uniform circular array (SUCA). These are realized by scanning one antenna element, allowing us to avoid the complex calibration procedure due to the mutual coupling of antenna array. The configuration of the antenna aperture is arbitrary and depends on the antenna scanning equipment. VNA measures each one of the transfer function of MIMO channel produced by SURA and SUCA.

Taking into account that it takes much time to move antennas and some accuracy is required in antenna alignment, this system uses a X-Y positioner, a rotator for antenna scanning and GPIB to control them as well as data extraction from VNA where we can achieve completely automatic measurement. This drastically reduces the measurement time while retaining the accuracy of antenna alignment. Note that antenna misalignment may cause a significant error in estimation result. This system is shown to derive reliable results of time-invariant channels while retaining reproducibility.

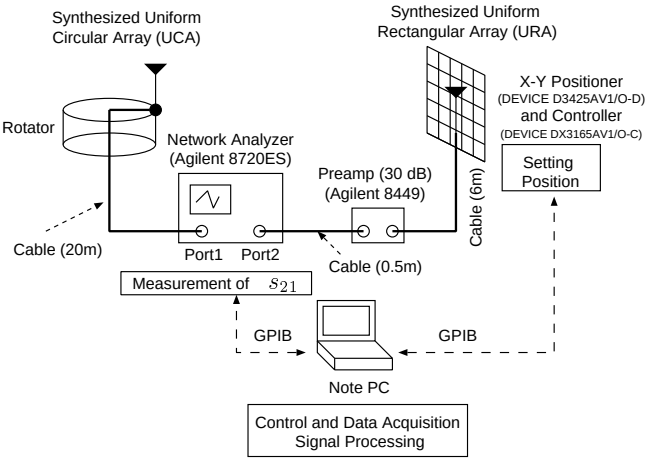

Fig. 1. Automatic MIMO Channel Measurement System

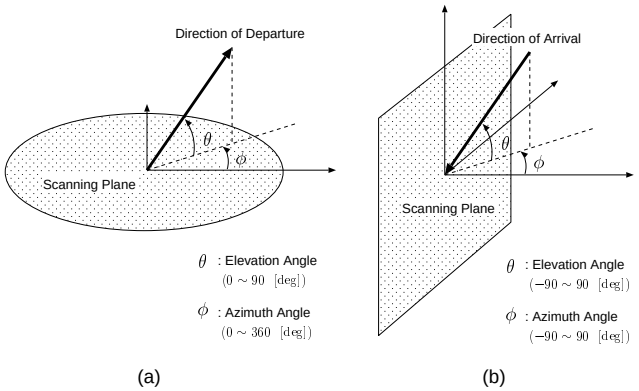

Fig. 2. Definition of Angles: (a) Tx (SUCA), (b) Rx (SURA).

III. ISI-SAGE Algorithm Implementation

ISI-SAGE algorithm[3] divides measured data into signal components and derives all the parameters of the paths jointly. This algorithm is essentially based on Maximum Likelihood Estimation (MLE) and shows a high resolution property as ESPRIT, but is rather flexible in terms of array configuration and easy to expand for joint estimation. In our study, the dimension of simultaneous search in MLE is $5L$ where L is number of estimated paths and excessive in computation. However, EM algorithm[5] estimates the complete data from incomplete data and SAGE algorithm introduce a search over hidden data space which reduces the search into one-dimension[6].

A. Data Model

Here we formulate a model for measured data in order to apply ISI-SAGE algorithm. We define SUCA as Tx and SURA as Rx to simplify notation. Suppose there are L plane waves radiating from Tx and impinging at Rx. Each wave has DOD $\mathbf{\Omega}_{l\mathrm{dep}} = [\phi_{l\mathrm{dep}}, \theta_{l\mathrm{dep}}]$, DOA $\mathbf{\Omega}_{l\mathrm{arr}} = [\phi_{l\mathrm{arr}}, \theta_{l\mathrm{arr}}]$, TOA τ_l and the variation of complex amplitude during the antenna and space propagation s_l $(1 \le l \le L)$. ϕ and θ denotes the azimuth and elevation angle and are defined as Fig. 2 at Tx and Rx, respectively.

In SUCA, antenna scanning is performed N_1 times with interval of $\Delta_c = 2\pi/N_1$ [rad]. In SURA, antenna scanning is performed both in azimuth and elevation direction with intervals of Δ_x and Δ_y and the number of steps are N_2 and N_3. At each channel measurement, we carry out N_4 points of transfer function sampling with sampling interval Δ_f and center frequency f_c. If the electrical length of the aperture size of antenna array is small enough to be assumed constant within the bandwidth, the measured data y_{k_1,k_2,k_3,k_4} can be expressed as

$$y_{k_1,k_2,k_3,k_4} = \sum_{l=1}^{L} \left[s_l \prod_{r=1}^{4} e^{j\mu_l^{(r)}(k_r)} \right] + n_{k_1,k_2,k_3,k_4} \qquad (1)$$

where $0 \le k_r \le (N_r - 1)$ $(1 \le r \le 4)$ indicates a index number of each sampling. s_l is a transfer function between phase reference point of Tx and that of Rx. n_{k_1,k_2,k_3,k_4} is a white gaussian noise of zero mean. s_l and $\mu_l^{(r)}(k_r)$ is denoted by

$$\begin{aligned}
s_l &= \alpha_l f_{\mathrm{dep}}(\mathbf{\Omega}_{l\mathrm{dep}}) f_{\mathrm{arr}}(\mathbf{\Omega}_{l\mathrm{arr}}), && (2)\\
\mu_l^{(1)}(k_1) &= \frac{2\pi}{\lambda} r \cos\theta_{l\mathrm{dep}} \cos\left(\phi_{l\mathrm{dep}} - k_1\Delta_c\right), && (3)\\
\mu_l^{(2)}(k_2) &= \frac{2\pi}{\lambda} k_2 \Delta_x \sin\phi_{l\mathrm{arr}} \cos\theta_{l\mathrm{arr}}, && (4)\\
\mu_l^{(3)}(k_3) &= \frac{2\pi}{\lambda} k_3 \Delta_y \sin\theta_{l\mathrm{arr}}, && (5)\\
\mu_l^{(4)}(k_4) &= 2\pi k_4 \Delta_f \tau_l, && (6)
\end{aligned}$$

where f_{dep} and f_{arr} are complex element patterns of Tx and Rx antenna element respectively, and α_l is a complex gain of the path. With ISI-SAGE algorithm, we want to estimate $5L$ propagation parameters that are contained in each $\mu^{(r)}$.

For simplicity, we vectorize the data defined in Eq. (7) as

$$\begin{aligned}
\mathbf{y} &= \begin{bmatrix}
y_{0,0,0,0} \\ y_{0,0,0,1} \\ \vdots \\ y_{0,0,0,N_4-1} \\ y_{0,0,1,0} \\ \vdots \\ y_{0,0,N_3-1,N_4-1} \\ y_{0,1,0,0} \\ \vdots \\ y_{0,N_2-1,N_3-1,N_4-1} \\ y_{1,0,0,0} \\ \vdots \\ y_{N_1-1,N_2-1,N_3-1,N_4-1}
\end{bmatrix} \in C^N \\
&= \mathbf{A}\mathbf{s} + \mathbf{n}, \qquad (7)
\end{aligned}$$

where $\mathbf{s} \in C^L$ and $\mathbf{n} \in C^N$ $(N = N_1N_2N_3N_4)$ are the complex amplitude vector and noise vector. $\mathbf{A} \in C^{N\times L}$ is a multi-dimensional phase difference matrix which can be expressed as follows.

$$\mathbf{A} = \mathbf{A}(\mu^{(1)}) \diamond \mathbf{A}(\mu^{(2)}) \diamond \mathbf{A}(\mu^{(3)}) \diamond \mathbf{A}(\mu^{(4)}) \in C^{N\times L} \qquad (8)$$

Note that $\diamond$ denotes the kronecker product of each row of the matrix and

$$\mathbf{A}(\mu^{(r)}) = \left[\mathbf{a}(\mu_1^{(r)}) \cdots \mathbf{a}(\mu_L^{(r)})\right] \in C^{N_r\times L}, \qquad (9)$$

$$\mathbf{a}(\mu_l^{(r)}) = \left[1 \; e^{j\mu_l^{(r)}(1)} \cdots e^{j\mu_i^{(r)}(N_r-1)}\right]^T \in C^{N_r}. \qquad (10)$$

B. SAGE Algorithm

By using the notation expressed in Eq. (7), cost function $z(\mathbf{\Omega}_{\mathrm{arr}}, \mathbf{\Omega}_{\mathrm{dep}}, \tau, \mathbf{x}_l)$ in EM algorithm becomes a following modified log-likelihood function

$$z(\mathbf{\Omega}_{\mathrm{dep}}, \mathbf{\Omega}_{\mathrm{arr}}, \tau, \mathbf{x}_l) = E[\mathbf{a}^H \mathbf{x}_l] \qquad (11)$$

where $\mathbf{x}_l$ is the complete data for lth wave and $\mathbf{a}$ is the phase difference vector that composes $\mathbf{A}$ in Eq. (7). Plane wave approximation was considered in conjunction with narrowband

approximation to derive Eq. (11). Then SAGE algorithm is executed iteratively in the following manner.

$$\begin{aligned}
\hat{\phi}_{l\mathrm{dep}} &= \arg\max_{\phi_{\mathrm{dep}}} \mid z(\phi_{\mathrm{dep}}, \theta_{l\mathrm{dep}}, \phi_{l\mathrm{arr}}, \theta_{l\mathrm{arr}}, \tau_l, \mathbf{x}_l) \mid \\
\hat{\theta}_{l\mathrm{dep}} &= \arg\max_{\theta_{\mathrm{dep}}} \mid z(\hat{\phi}_{l\mathrm{dep}}, \theta_{\mathrm{dep}}, \phi_{l\mathrm{arr}}, \theta_{l\mathrm{arr}}, \tau_l, \mathbf{x}_l) \mid \\
\hat{\phi}_{l\mathrm{arr}} &= \arg\max_{\phi_{\mathrm{arr}}} \mid z(\hat{\phi}_{l\mathrm{dep}}, \hat{\theta}_{l\mathrm{dep}}, \phi_{\mathrm{arr}}, \theta_{l\mathrm{arr}}, \tau_l, \mathbf{x}_l) \mid \\
\hat{\theta}_{l\mathrm{arr}} &= \arg\max_{\theta_{\mathrm{arr}}} \mid z(\hat{\phi}_{l\mathrm{dep}}, \hat{\theta}_{l\mathrm{dep}}, \hat{\phi}_{l\mathrm{arr}}, \theta_{\mathrm{arr}}, \tau_l, \mathbf{x}_l) \mid \\
\hat{\tau}_l &= \arg\max_{\tau} \mid z(\hat{\phi}_{l\mathrm{dep}}, \hat{\theta}_{l\mathrm{dep}}, \hat{\phi}_{l\mathrm{arr}}, \hat{\theta}_{l\mathrm{arr}}, \tau, \mathbf{x}_l) \mid
\end{aligned}$$

The gain of each path corresponds to the maximum output of cost function,

$$P_l = \frac{1}{\mid \mathbf{a}_l \mid^2} \mid z(\hat{\mathbf{\Omega}}_{l\mathrm{dep}}, \hat{\mathbf{\Omega}}_{l\mathrm{arr}}, \hat{\tau}_l, \mathbf{x}_l) \mid^2 . \qquad (12)$$

C. Initialization and Search Procedure

SAGE algorithm does not always yield a global optimum solution. Since the method of initialization and search directly affects the reliability of the results, we have to seek an optimum way of managing SAGE algorithm in many aspects. What we have to consider is as follows:

Problem of Spurious Paths (Leakage) : We can often see undesired results that are unable to identify to real channel. Sprious paths themselves are sometimes equivalent to the sidelobe occured in the process of fourier analysis and they may be easily detected especially in detection of weaker path. To overcome this problem, these methods are possible :

- Increment of simultaneous search dimension : The appearance of spurious paths are a cost of reducing the load of calculation by dividing the search space. Therefore, increment of simultaneous search dimension can be an effective solution to avoid spurious paths. This should be performed by considering the trade off between the load of calculation and high dimensionality.
- Data windowing[7]: By multipling the appropriate window function to some part of the parameter domain, we can decrease the sidelobe level. However at the same time, this method cannot avoid the decrement of data signal to noise ratio and intrinsic resolution of the algorithm.

Divergence of Power : In the iteration process, parallel updating procedure may cause a divergence of power. Based on [3], the notion of SIC (Succesive Interference Cancellation) may be a very strong tool for avoiding this phenomenon.

Taking into account the above consideration, we choose a search procedure depicted in Fig. 3. This method is applicable when the number of samples over frequency and space domains are sufficiently large. The process is a combination of local search based on SAGE algorithm and global mesh search based on EM algorithm. In global mesh search, we aim at the region which may include a maximum point of the cost function. After that, local search is carried out inside the selected region and find an accurate peak. The parameters estimation procedure is divided into two steps, $[\phi_{l\mathrm{arr}}, \theta_{l\mathrm{arr}}, \tau_l]$ step and $[\phi_{l\mathrm{dep}}, \theta_{l\mathrm{dep}}]$ step with re-estimation of the parameters of previous step. Note that this method is also based on the SIC and repeated until the number of detected paths reaches the predefined number of waves or the detected path level falls below the noise floor level.

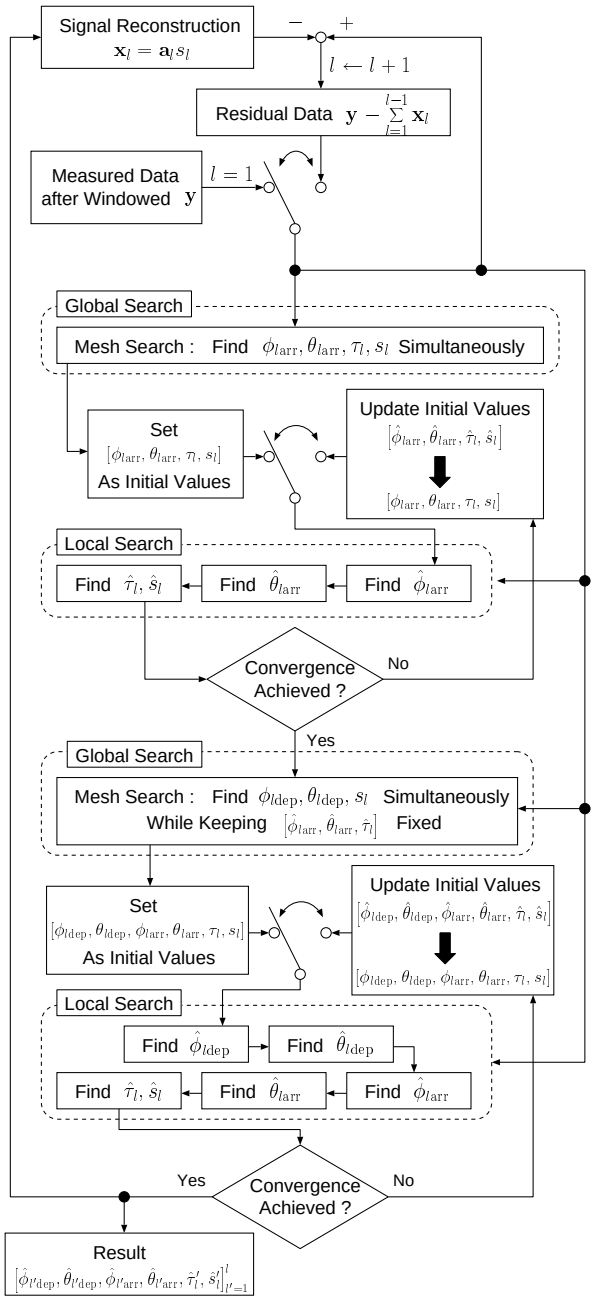

Fig. 3. Implementation of ISI-SAGE Algorithm

D. Dual Polarized Estimation

We propose a method which estimates a polarization characteristics of an identical path with SAGE algorithm. Specifically, the data was taken from dual othogonal polarized wave in the measurement and they are applied to SAGE algorithm where we maximize their likelihood at simultaneous search. If the modified log-likelihood function for each polarization is denoted as $z_1(\mathbf{\Omega}_{\rm dep}, \mathbf{\Omega}_{\rm arr}, \tau, \mathbf{x}_l)$, $z_2(\mathbf{\Omega}_{\rm dep}, \mathbf{\Omega}_{\rm arr}, \tau, \mathbf{x}_l)$, then the cost function for this estimation becomes

$$z(\mathbf{\Omega}_{\rm dep}, \mathbf{\Omega}_{\rm arr}, \tau, \mathbf{x}_l) = |z_1(\mathbf{\Omega}_{\rm dep}, \mathbf{\Omega}_{\rm arr}, \tau, \mathbf{x}_l)|^2 + |z_2(\mathbf{\Omega}_{\rm dep}, \mathbf{\Omega}_{\rm arr}, \tau, \mathbf{x}_l)|^2. \quad (13)$$

In the derivation of Eq. (13), it is considered that the square of modified log-likelihood function corresponds to the gain of each path. Consequently, the path gain for different polarization but identical path can be obtained by this method as

$$P_{li} = \frac{1}{|\ \mathbf{a}_l\ |^2}\ |\ z_i(\hat{\mathbf{\Omega}}_{l\rm dep}, \hat{\mathbf{\Omega}}_{l\rm arr}, \hat{\tau}_l, \mathbf{x}_l)\ |^2 \quad (i = 1, 2). \quad (14)$$

This process provide us with an accurate insight of polarization characteristics of each path.

IV. Measurement Campaign

We performed a measurement campaign in indoor NLOS channel by using the system we propose. The environment is depicted in Fig. 4. In Fig. 4, Tx, Rx antennas are depicted at the centers of the spatial scanning and we can find some small pillars at the wall between the corridor and the room.

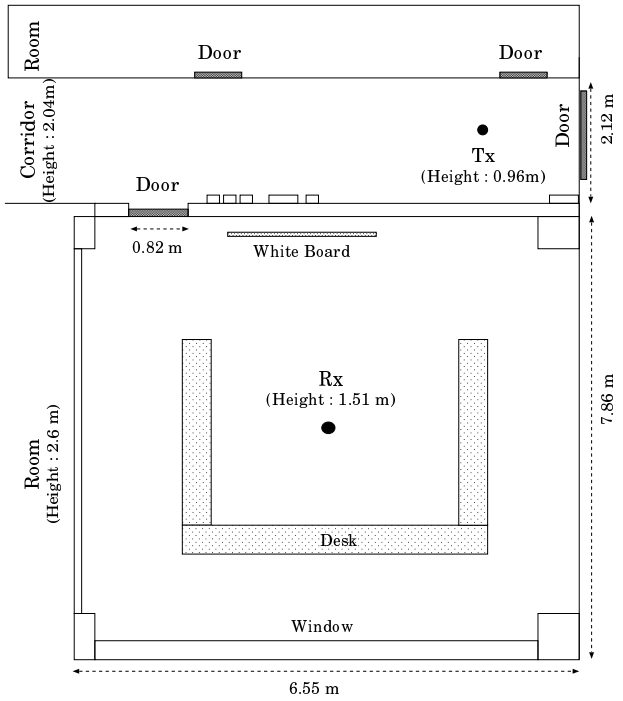

Fig. 4. Environment of the Measurement Campaign

The way of channel parameterization obeys the description in section III-A. Measurement was conducted with both

TABLE I
Specification of the Measurement and Signal Processing

Measurement points	URA: Spatial 7×7 points (Interval 25 [mm]), UCA: 10 points with radius 20 [mm]. Transfer function sampling: 21 points from 5.8 [GHz] to 5.9 [GHz].
Estimated Parameters	DOD azimuth, elevation, DOA azimuth, elevation, TOA, Path gain.
Antennas	Standard dipole antenna whose reflection coefficient is below -10 [dB] in $5.8 \sim 5.9$ [GHz] in both Tx, Rx.
Calibration	Use calibration function of VNA.
Snapshot	20 times.
Signal Processing	ISI-SAGE algorithm based on the process of Fig. 3 where rectangular windowing and dual polarized maximization was performed.
Polarization	Vertical-Vertical(VV), Horizontal-Horizontal(HH).
The number of waves	20.

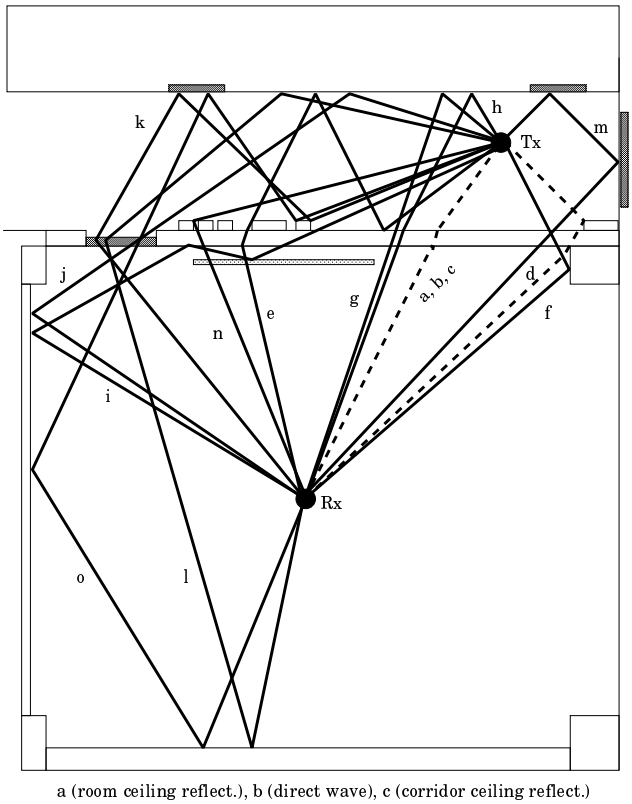

a (room ceiling reflect.), b (direct wave), c (corridor ceiling reflect.)

Fig. 5. Result of Path Identification

TABLE II

RESULT OF THE SIGNAL PROCESSING WITH DUAL POLARIZED ESTIMATION

	Result of identification	VV meas. path gain [dB]	HH meas. path gain [dB]
a	Wall penetrat. Room ceiling reflect.	-105.66	-84.93
b	Wall penetrat. (the shortest path)	-87.75	-87.60
c	Corridor ceiling reflect. Wall penetrat.	-92.81	-84.83
d	Wall penetrat. Corridor pillar diffract.	-87.24	-90.79
e	Twice wall reflect. in corridor / Wall & whiteboard penetrat.	-97.66	-104.36
f	Wall penetrat. Room pillar reflect.	-100.20	-93.06
g	Corridor wall reflect. & penetrat.	-94.26	-91.15
h	Corridor wall reflect. & penetrat. Room floor reflect.	-100.89	-95.71
i	Wall penetrat. Whiteboard reflect. Twice room wall reflect.	-102.96	-100.15
j	Corridor wall reflect. Door penetrat. Room wall reflect.	-97.19	-106.98
k	Corridor pillar diffract. Corridor door reflect. Door penetrat.	-98.65	-102.55
l	Corridor wall reflect. Door penetrat. Room window reflect.	-100.19	-105.76
m	Twice door reflect. in corridor / Wall penetrat.	-101.38	-103.88
n	Corridor pillar diffract. Wall penetrat.	-102.62	-104.22
o	Corridor pillar diffract. Corridor door reflect. Door penetrat./ Room wall & window reflect.	-104.14	-99.48

vertical and horizontal polarized waves for dual polarized estimation. It should be pointed out that the antenna element positioning was peformed so as not to change the directivity within the array. In Table I, specifications of the measurement and signal processing are presented. Note that the process "calibration" is the one that removes the transfer function of cables, LNA, and connectors from the measured data which results in extracting only spatial transfer function.

Results of the signal processing and identification to real environment are shown in Table II and Fig. 5. In Fig. 5, the path expressed in dashed line indicates the dominant one whose gain is above -90 [dB]. They are wall-penetrated waves including the shortest delay path. All the other paths have gains below -90 [dB], but we can find many waves penetrated or diffracted from the door, walls and pillar. Note that we also obtain long delayed paths which were unable to identify to real channel and some spurious paths that are not mentioned in Table II. However, it was confirmed that the number of spurious paths in the results decreased when the dual polarization maximization was employed compared to the single polarization estimation. Herein spurious paths mean that the direction of departure or arrival converged to the endfire direction seen from the antenna aperture where the accuracy of the estimation seriously degrades.

V. CONCLUSION

This report represent an easily integrated channel sounding system with VNA, X-Y positioner, and rotator which perform a double directional measurement for time invariant channel. The system achieves a completely automatic measurement while retaining accuracy. In signal processing, we employ ISI-SAGE algorithm and showed one of the realization of initialization and search procedure in conjunction with the dual polarized estimation. The algorithm is especially effective when the number of sampling points is large. In NLOS indoor environment estimation, we assessed the efficiency of this system and we detected many waves including dominant paths as well as long delayed paths and many propagation phenomena. Also it was confirmed that the dual polarized estimation affects the derivation of stable result.

The data which was measured by our system provides a very interesting insight towards the analysis of propagation phenomena as well as MIMO transmission system. The deterministic approach in this report offers parameters of each propagation path so that we can analyze the propagation phenomena separately : penetration, reflection, diffraction and so on. On the contrary to such a microscopic analysis, macroscopic analysis, such as MIMO channel modelling based on statistic approach are also possible.

REFERENCES

[1] K. Sakaguchi, J. Takada, and K. Araki, "A Novel Architecture for MIMO Spatio-Temporal Channel Sounder", *IEICE Trans. Electron.*, Vol. E85–C, No. 3, pp. 436–441, Mar. 2002.

[2] R. S. Thomä, D. Hampicke, A. Richter, G. Somerkorn, A. Schneider, U. Trautwein, and W. Wirnitzer, "Identification of Time-Variant Directional Mobile Radio Channels", *IEEE Trans. Instrum. and Meas.*, Vol. 49, No. 2, pp. 357–364, Apr. 2000.

[3] B. H. Fleury, X. Yin, K. G. Rohbrandt, P. Jourdan, and A. Stucki, "Performance of a High-Resolution Scheme for Joint Estimation of Delay and Bidirection Dispersion in the Radio Channel", in *Proc. IEEE 55th Veicular Technology Conference (VTC 2002/Spring)*, May 2002.

[4] K. Haneda, J. Takada, T. Iwata, and Y. Wakinaka, "Construction of a Propagation Path Determination System for Short Range Wireless Communication System", in *Proc. 3rd International Workshop on ITS Telecommunications (ITST2002)*, pp. 289–294, Seoul, Korea, Nov. 2002.

[5] A. P. Dempster, N. M. Laird, and D. B. Rubin, "Maximum Likelihood from Incomplete Data via the EM Algorithm", *J. Royal Statist. Soc., Ser.B*, Vol. 39, No. 1, pp. 1–38, 1977.

[6] J. A. Fessler and A. O. Hero, "Space-alternating Generalized Expectation Maximization Algorithm", *IEEE Trans. Signal Processing*, Vol. 42, pp. 2664–2677, Oct. 1994.

[7] C. C. Chong, D. I. Laurenson, C. M. Tan, S. McLaughlin, M. A. Beach and A. R. Nix, "Joint Detection-Estimation of Directional Channel Parameters Using the 2-D Frequency Domain SAGE Algorithm with Serial Interference Cancellation", in *COST 273 Temporary Document*, TD(02)026, Espoo, Finland, May 2002.

* This manuscript is pending for approval by PIMRC 2003, Beijin, China.